THE JOURNAL OF PHYSICAL CHEMISTRY B

 VOLUME 105, NUMBER 50, DECEMBER 20, 2001

LETTERS

Relation between Particle Coordination Number and Porosity in Nanoparticle Films: Implications to Dye-Sensitized Solar Cells

Jao van de Lagemaat,* Kurt D. Benkstein, and Arthur J. Frank*

National Renewable Energy Laboratory, Golden, Colorado 80401

Received: August 30, 2001; In Final Form: October 23, 2001

The morphology and local three-dimensional structure of mesoporous nanoparticle TiO_2 films are simulated by using a simple method based on the random packing of spheres. The pore size distribution in the film that is predicted by the simulations is in excellent concurrence with experimental data. The spatial distribution of particles appears essentially random outside of the first shell of nearest neighbors. The average coordination number of particles depends strongly on film porosity. For compact films (40% porosity), the average coordination number is about 6.6, whereas for open-structured films (80% porosity), the average number of particle interconnections is as low as 2.8. At porosities (50−65%) typically present in nanocrystalline TiO_2 films employed in dye-sensitized solar cells, the simulations indicate that each particle is, on average, in contact with 4 or 5 others. However, the distribution of coordination numbers is broad. The implication of such highly branched particle structures on electron transport is discussed.

Introduction

Semiconductor structures at the nanometer scale (1−100 nm) have received intense scrutiny for possible electrochemical and photochemical applications, such as sensors,[1] photocatalysts,[2,3] batteries,[4,5] photochromics,[6−8] electrochromics,[9,10] and solar cells.[11−16] Current interest in the study of photochemical solar cells has centered on dye-sensitized mesoporous nanocrystalline TiO_2. The most extensively studied cell consists of a dye-covered anatase TiO_2 film (ca. 10−15 μm thick), sandwiched between two transparent electrodes.[16] The film consists of a large network of interconnected particles about 20 nm in diameter. The film porosity is typically in the range of 50−65%,[17] implying that pores constitute more than half of the volume of the film. Because of the porous nature of the film, the redox electrolyte permeates the entire structure and is in contact with the nanoparticles. The TiO_2 network is the recipient of injected electrons from optically excited dye molecules and provides the conductive pathway from the site of electron injection to the collecting electrode. The redox species in the electrolyte transports the hole from the oxidized dye to the counter electrode. At one-sun light intensity, the time constant for the collection of injected electrons in nanocrystalline films is several orders of magnitude slower than it is in single crystalline TiO_2. Time-resolved [18−25] and theoretical [26,27] studies suggest that the slow collection is due to trap-limited transport. Computer simulations, based on a random-walk approach and trap-limited transport, reproduce fully photocurrent transient data under the normal working conditions of dye-sensitized solar cells.[23] A key assumption of this model is that electrons can move from trap to trap in any one of six fundamental directions in a three-dimensional lattice. An important implication of this assumption is that film morphology does not limit the collection of electrons. This means that at the present level of film porosity (50−65%) there are a sufficient number of interparticle connections (contacts) in the network for electrons to move readily from particle to particle without significant impediment. There is only sparse quantitative information in the literature about the coordination number of particles in nanostructured films and

10.1021/jp013369z CCC: $20.00
Published on Web 11/27/2001

how porosity affects it. At the limit of dense random packing, corresponding to a porosity of 36%, it has been shown[28] that the coordination number is quite high, about 7.4.[29,30] It is expected that increasing the film porosity will decrease the average coordination number or number of interparticle connections.[31] Understanding quantitatively the relation between film porosity and the coordination number of individual particles in the network is important for gaining a comprehensive knowledge of the morphological factors that can affect photocarrier transport and recombination in the solar cell.

In this paper, we investigate the relation between film porosity and the local three-dimensional particle structure of nanoporous films using a simple computer method to simulate nanoparticle films. Information on the coordination number of particles and the distribution of pore sizes is obtained. The distribution of pore sizes in the film that is predicted by the simulations is found to be in excellent agreement with experimental data. The methodology developed in this paper is readily applicable to any nanoparticle films that are composed of randomly stacked and approximately spherically shaped particles (e.g., quantum dots).

Experimental Section

Computer Simulations. An optimization procedure is used to simulate mesoporous nanoparticle films. Particles that make up the film are placed on random locations inside a three-dimensional box. The spatial arrangement of the particles is then optimized by using a function that considers only interaction of a particle with its first and second nearest neighbors. When a particle infringes on the same space of a nearest neighbor, it is repelled with a constant force. To ensure film continuity, each particle is required to be in contact with at least two neighbors such that an isolated particle is drawn into the coordinating sphere of the two closest neighbors, corresponding to the average distance between them. Sintering of a film, to bring the particles into electrical contact, is simulated by requiring the distance between two nearest neighbors to be slightly less than twice their radius (ca. 2.5% encroachment, corresponding to a 10% loss of surface area for four-coordinated spheres). The final position of a particle would correspond physically to a location where attractive and repulsive forces between neighboring particles are equal and opposite. Coordination numbers are determined by calculating the radial distribution function for each particle and integrating the peak obtained at $2r$.

The porosity is determined by averaging the void volume of several cross-sectional slices of a film. A distribution of pore sizes is obtained by a Monte Carlo method. Spheres of a certain size are placed randomly in the pores. The number of times spheres of a particular radius can fill the pores of a film without contacting a particle is proportional to the volume of pores with a radius equal to or greater than the radius of the spheres. This procedure, when repeated for a wide range of different-sized spheres, yields a pore size distribution. All calculations were performed using either Igor Pro (Wavemetrics, Inc.) or a C++ program running on a PowerPC G4 computer.

Sample Preparation and Measurements. Anatase nanocrystals (~19 nm in diameter) were prepared and analyzed by X-ray diffraction (XRD) as described elsewhere.[14,15,32] Particle size was estimated from the Scherrer equation: $L = 0.9\lambda/(B(2\theta)\cos(\theta))$, where L is the crystallite size and $B(2\theta)$ is the line width. TiO_2 films were deposited on glass substrates, annealed at 450 °C, and then scraped off to give a powder suitable for gas sorption studies.

Nitrogen adsorption−desorption isotherms were obtained using a Quatachrome NOVA 2000 high-speed gas sorption surface and pore size analyzer. The samples were outgassed at 250 °C for 3 h under vacuum before beginning sorption studies at 77 K. Desorption data were analyzed using the BJH (Barrett, Joyner, and Halenda) method for cumulative pore volume and pore volume distribution (Autosorb 1 for Windows, version 1.20, Quantachrome Corporation). The film porosity was estimated by dividing the cumulative pore volume per gram by the sum of the pore volume per gram and the inverse of the density of anatase TiO_2 (0.257 cm^3/g). Film morphology was investigated by field emission scanning electron microscopy (SEM; JEOL model 6320F).

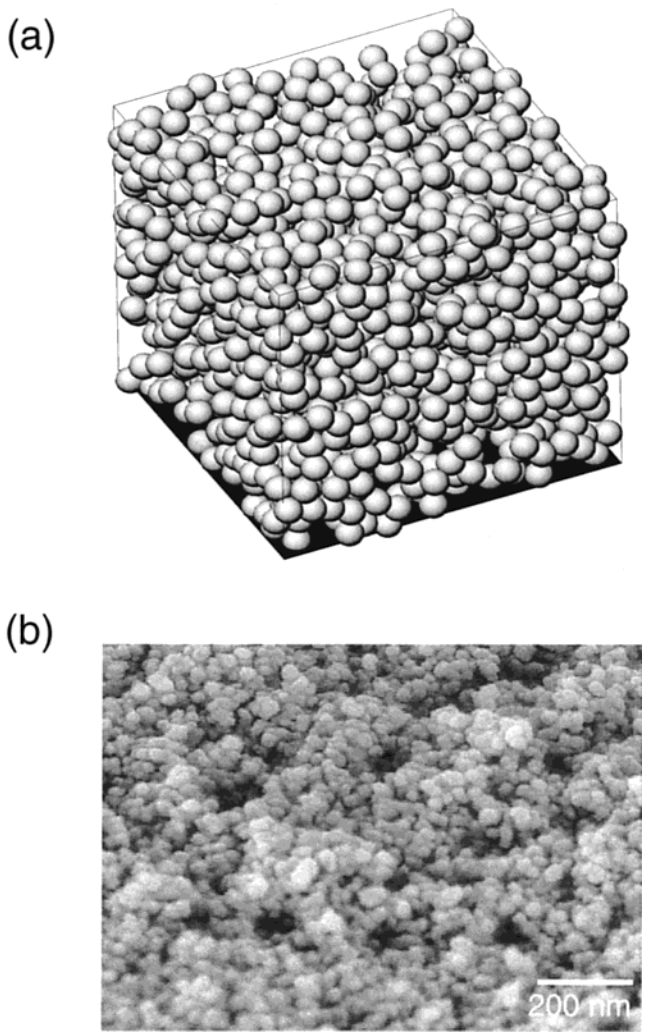

Figure 1. A three-dimensional representation of a simulated nanoparticle film having a porosity of 55% (a) and SEM plain-view image of a nanocrystalline TiO_2 film (b).

Results and Discussions

Figure 1 shows a three-dimensional representation of a simulated film together with a plain-view SEM image of a nanocrystalline TiO_2 film. It can be seen in the SEM micrograph that the TiO_2 anatase film is, as is well-established, composed of nanoparticles of approximately spherical shape with no apparent long-range order. The micrograph shows the near-surface region of the film. The simulation depicts a more depth-of-field view of the three-dimensional lattice. Although the visual perspectives of the films are different, the physical resemblance of the simulated film to the SEM image is remarkably close.

Figure 2 compares plots of the normalized simulated specific pore volume vs pore radius (normalized to the average particle

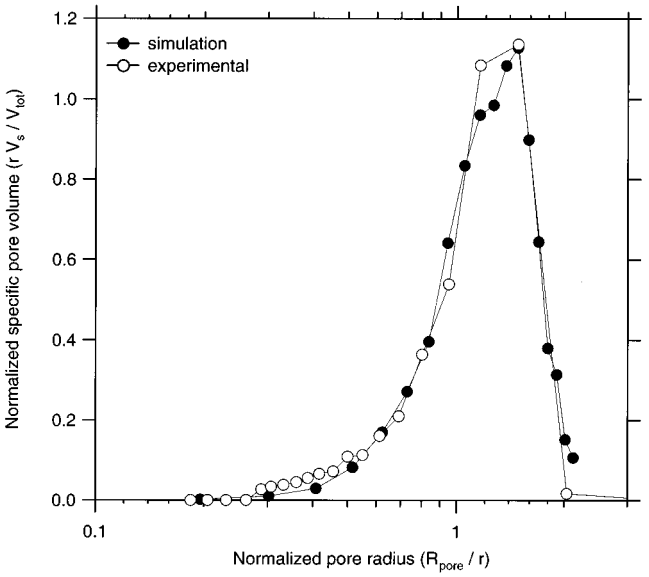

Figure 2. Dependence of normalized specific pore volume (rV_s/V_{tot}) on normalized pore radius (R_{pore}/r) for simulated and experimentally measured films having a porosity of about 60%. r is the average particle radius (~9.5 nm), V_s is the volume of a pore of radius R_{pore}, and V_{tot} is the total pore volume.

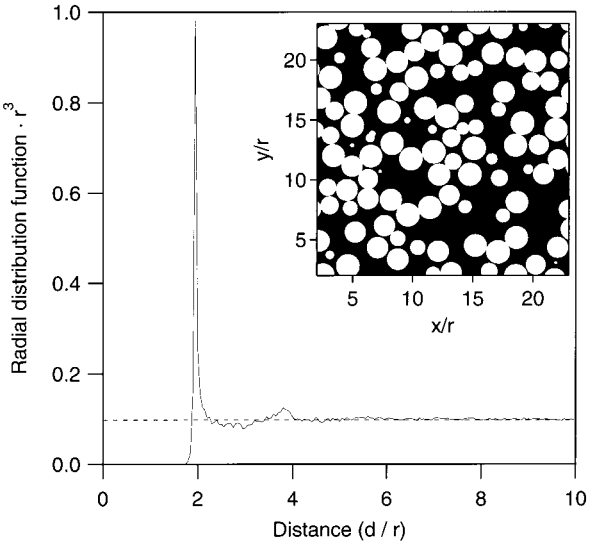

Figure 3. Dependence of the radial distribution function $\times$ r^3 (no. of particles/unit volume) on the distance, d, from the center of a particle for a film porosity, P, of 58%. The dashed line shows the form of the distribution function for completely randomly distributed particles (RDF $= 3(1 - P)/(4\pi r^3)$, where r is the particle radius).

radius (~9.5 nm)) for simulated and experimentally measured films having a porosity of about 60%. The excellent match of the simulation to the experimental data indicates that the model provides a very good description of the morphology of the nanoparticle film. The simulations predict, as is often observed,[16,17] that the most probable pore size in a film is somewhat (ca. 30−40%) larger than the average particle size and that about 80% of the pores are larger than the average particle size.

Figure 3 shows a plot of the radial distribution function vs the radial distance (normalized to the particle radius) from the center of a particle in a film having a porosity of about 60%. If the spatial distribution of particles were completely random, the radial distribution function would have a constant value (dashed line), regardless of the distance from a particle. The presence of several peaks in the plot indicates short-range order. The intense peak at 2r shows that the first shell of nearest

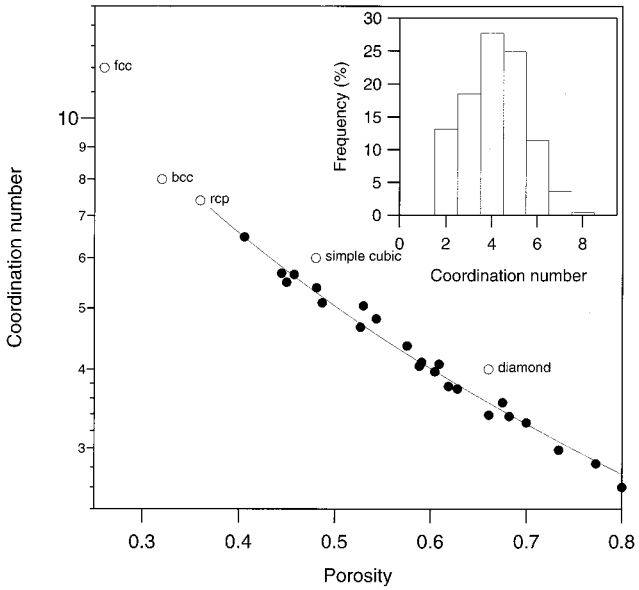

Figure 4. Dependence of the average coordination number on film porosity (filled circles). The open circles designate basic monatomic "crystal" structures. The inset shows the distribution of coordination numbers associated with a film porosity of 58%. Sintering of the film is simulated by requiring the distance between two nearest neighbors to be slightly less than twice their radius (ca. 2.5% encroachment).

neighbors surrounding a particle is strongly correlated, indicating, as required by the model, that essentially each particle in the film is in direct contact with at least one other. The presence of faint peaks at 3.5r and 5r, corresponding to a second and third coordination shell, indicates very weak correlation. Thus, outside of the first shell, the spatial distribution of particles is essentially random. From the integration of the peak at 2r, it is estimated that the average coordination number of a particle in the film is 4. The positions of the peaks at 3.5r and 5r are also consistent with the particles having an average coordination number of about 4. Assuming 4-fold coordination, simple geometry arguments place the first particle coordination shell at 3.46r and the second shell at 4.90r, which is in excellent agreement with the prediction of the model. The inset in Figure 3, which depicts a cross sectional view of a simulated film, shows the relative magnitude of the void volume surrounding the particles and the extent to which particles appear within the same plane.

Figure 4 shows a strong relation between film porosity and the average coordination number of the nanoparticles. When the film porosity increases from 40% to 80%, the average coordination number of a particle decreases from about 6.6 to 2.8. No results are shown for porosities smaller than 40% because the present computer model is not able to optimize structures in this porosity range within a reasonable computation time. It is also worthwhile to point out that a porosity of 36% is the smallest possible porosity for randomly stacked spheres.[28] Figure 4 also displays the coordination numbers of several basic monatomic crystal structures and that of the random *closed* packed (rcp) structure.[29,30] The coordination numbers of the random structures follow loosely the graph for the simple crystal structures. The simple cubic structure has a relative porosity (void volume) of 48% and a coordination number of 6. At the same porosity, the simulated structures have an average particle coordination number of 5.3. Hence, a cubic lattice is a reasonable approximation for a film having a porosity of about 50%. The relation between porosity and coordination numbers in Figure 4 reveals that random-structured films have, in general, lower

coordination numbers than simple crystal structures at the same porosity. A random-structured film with a porosity of 60% has an average particle coordination number of 4 (cf. Figure 3). This coordination number corresponds to the diamond structure, which has a porosity (void volume) of 66%. A film with a porosity of 75% has a coordination number of only 3, illustrating the extent to which the number of interparticle contacts drops off at higher porosities. For a particle network to be mechanically stable, the average coordination number has to be at least 3,[29] implying that free-standing (randomly stacked) nanoparticle films with porosities higher than 75% are probably physically unattainable. From Figure 4, an approximate relationship between coordination number (N) and porosity (P) can be obtained.

$$N = \frac{3.08}{P} - 1.13 \qquad (1)$$

This relation is plotted in Figure 4.

The inset in Figure 4 shows the distribution of coordination numbers associated with a film porosity of 58%, which is within the range of porosities (50−65%) typically measured for TiO_2 films used in dye-sensitized solar cells. It can be seen that most particles have 3−5 nearest neighbors. Less than 14% of the total number of particles have less than 3 nearest neighbors, and 0.5% of them have as many as 8 nearest neighbors. On average, particles have a coordination number of 4.2, indicating that the nanostructured film is highly branched. From the perspective of electron transport, a coordination number of about 4 implies that an electron residing on a particular particle has 4 possible directions in which it can move to an adjoining particle. It follows that *if* electron transport is trap-limited,[18−26] an average coordination number or branching number of 4.2 provides a sufficient number of pathways for electrons to move from particle to particle without being spatially constrained by the morphology of the nanoparticle network.

Conclusions

A simple computer method based on the random packing of spheres was used to simulate the morphology and local structure of mesoporous nanoparticle TiO_2 films. The distribution of pore sizes in the film that is predicted by the simulations is found to be in excellent agreement with experimental data. Outside of the first shell of nearest neighbors, the spatial distribution of particles appears essentially random. The random-structured films have, in general, lower particle coordination numbers than corresponding simple periodic particle lattices at the same porosity. A strong relation between film porosity and the average coordination number of the nanoparticles is found. For film porosities of 40−80%, the average coordination number of a particle ranges from about 6.5 to 2.8. At film porosities (50−65%) typically present in nanocrystalline TiO_2 films used in dye-sensitized solar cells, each particle is found to be in contact with 4 or 5 others on average, indicating that the nanostructured film is highly branched. The effect of such a highly branched particle structure on electron transport is discussed.

Acknowledgment. This work was supported by the Office of Science, Division of Chemical Sciences, and the Office of Utility Technologies, Division of Photovoltaics, U.S. Department of Energy, under Contract No. DE-AC36-99GO10337.

References and Notes

(1) Doron, A.; Joselevich, E.; Schlittner, A.; Willner, I. *Thin Solid Films* **1999**, *340*, 183.
(2) Huang, Z.; Maness, P. C.; Blake, D. M.; Wolfrum, E. J.; Smolinski, S. L.; Jacoby, W. A. *J. Photochem. Photobiol. A* **2000**, *130*, 163.
(3) Grätzel, M.; Frank, A. J. *J. Phys. Chem.* **1982**, *86*, 2964.
(4) Kavan, L.; Attia, A.; Lenzmann, F.; Elder, S. H.; Grätzel, M. *J. Electrochem. Soc.* **2000**, *147*, 2897.
(5) McGraw, J. M.; Perkins, J. D.; Zhang, J.-G.; Liu, P.; Parilla, P. A.; Turner, J.; Schulz, D. L.; Curtis, C. J.; Ginley, D. S. *Solid State Ionics* **1998**, *113*, 407.
(6) Bechinger, C.; Ferrere, S.; Zaban, A.; Sprague, J.; Gregg, B. A. *Nature* **1996**, *383*, 608.
(7) Pichot, F.; Ferrere, S.; Pitts, R. J.; Gregg, B. A. *J. Electrochem. Soc.* **1999**, *146*, 4324.
(8) Gregg, B. A. *Endeavour* **1997**, *21*, 52.
(9) Hagfeldt, A.; Vlachopoulos, N.; Grätzel, M. *J. Electrochem. Soc.* **1994**, *141*, L82.
(10) Lee, S.-H.; Cheong, M. H.; Tracy, C. E.; Mascarenhas, A.; Czanderna, A. W.; Deb, S. K. *Appl. Phys. Lett.* **1999**, *75*, 1541.
(11) Pehnt, M.; Schulz, D. L.; Curtis, C. J.; Jones, K. M.; Ginley, D. S. *Appl. Phys. Lett.* **1995**, *67*, 2176.
(12) O'Regan, B.; Grätzel, M. *Nature* **1991**, *353*, 737.
(13) Zaban, A.; Miçic, O. I.; Gregg, B. A.; Nozik, A. J. *Langmuir* **1998**, *14*, 3153.
(14) Park, N.-G.; Schlichthörl, G.; van de Lagemaat, J.; Cheong, H. M.; Mascarenhas, A.; Frank, A. J. *J. Phys. Chem. B* **1999**, *103*, 3308.
(15) Park, N.-G.; van de Lagemaat, J.; Frank, A. J. *J. Phys. Chem. B* **2000**, *104*, 8989.
(16) Barbé, C. J.; Arendse, F.; Comte, P.; Jirousek, M.; Lenzmann, F.; Shklover, V.; Grätzel, M. *J. Am. Ceram. Soc.* **1997**, *80*, 3157.
(17) Benkstein, K. D.; van de Lagemaat, J.; Frank, A. J. Unpublished results.
(18) Schwarzburg, K.; Willig, F. *Appl. Phys. Lett.* **1991**, *58*, 2520.
(19) Cao, F.; Oskam, G.; Meyer, G. J.; Searson, P. C. *J. Phys. Chem.* **1996**, *100*, 17021.
(20) de Jongh, P. E.; Vanmaekelbergh, D. *Phys. Rev. Lett.* **1996**, *77*, 3427.
(21) de Jongh, P. E.; Vanmaekelbergh, D. *J. Phys. Chem. B* **1997**, *101*, 2716.
(22) van de Lagemaat, J.; Frank, A. J. *J. Phys. Chem. B* **2000**, *104*, 4292.
(23) van de Lagemaat, J.; Frank, A. J. *J. Phys. Chem. B* **2001**, *105*, 11194.
(24) Kopidakis, N.; Schiff, E. A.; Park, N.-G.; van de Lagemaat, J.; Frank, A. J. *J. Phys. Chem. B* **2000**, *104*, 3930.
(25) Fisher, A. C.; Peter, L. M.; Ponomarev, E. A.; Walker, A. B.; Wijayantha, K. G. U. *J. Phys. Chem. B* **2000**, *104*, 949.
(26) Nelson, J. *Phys. Rev. B.* **1999**, *59*, 15374.
(27) Vanmaekelbergh, D.; de Jongh, P. E. *Phys. Rev. B* **2000**, *61*, 4699.
(28) Torquato, S.; Truskett, T. M.; Debenedetti, P. G. *Phys. Rev. Lett.* **2000**, *84*, 2064.
(29) Bouvard, D.; Lange, F. F. *Phys. Rev. A* **1992**, *45*, 5690.
(30) Mason, J. *J. Colloid Interface Sci.* **1971**, *35*, 75.
(31) Gotoh, K. *Nature* **1971**, *231*, 108.
(32) van de Lagemaat, J.; Park, N.-G.; Frank, A. J. *J. Phys. Chem. B* **2000**, *104*, 2044.